Effect of strain on the energetics and kinetics of dissociation of Sb_4 on Ge(001)

Jian-Tao Wang,[1,*] Changfeng Chen,[2] E. G. Wang,[1] Ding-Sheng Wang,[1] H. Mizuseki,[3] and Y. Kawazoe[3]
[1]*Beijing National Laboratory for Condensed Matter Physics, Institute of Physics, Chinese Academy of Sciences, Beijing 100080, China*
[2]*Department of Physics, University of Nevada, Las Vegas, Nevada 89154, USA*
[3]*Institute for Materials Research, Tohoku University, Sendai 980-8577, Japan*
(Received 13 June 2008; revised manuscript received 10 July 2008; published 11 August 2008)

A comprehensive search for the precursor dissociation of antimony tetramers on Ge(001) with strain was carried out using first-principles calculations. In contrast to previous theoretical studies on Si(001) [Phys. Rev. Lett. **97**, 046103 (2006)] and in agreement with recent experiments, we reveal a *square* intermediate anisotropy dissociation pathway across the surface dimer row, where the dissociation energetics and kinetics can be qualitatively altered by the strain and lead to divergent dissociation pathways and patterns with *substrate-dimer-bond breaking* due to the weak interactions between Ge-Ge and Sb-Ge bonds.

DOI: 10.1103/PhysRevB.78.073403 PACS number(s): 68.65.−k

It has long been known that molecular chemisorption on solid surfaces often involves intermediate precursor states and several competing dynamical processes such as dissociation, diffusion, and desorption.[1] A typical example is the reaction of group-V elements (e.g., As, Sb, and Bi) with Si and Ge surfaces.[2–18] For Sb_4 on Si(001), the three-dimensional (3D) clusters can convert to flat tetramers that can then split into pairs of dimers. Scanning tunneling microscopy (STM) measurements[2–4] and density-functional theory (DFT) calculation[14] revealed a *two-stage* reaction process involving two distinct pathways, *along* and *across* the surface dimer row via a *rhombus* intermediate state. Similar but distinct reaction behavior is also observed for Sb_4 on Ge(001) where STM measurements identified a pathway involving a two-dimensional (2D) *flat square* intermediate state across the surface dimer row.[5] Such processes have attracted considerable attention because they play a key role in the epitaxial growth of Ge/Si heterostructures.[15–18]

In this Brief Report, we present a comprehensive search on the dissociation energetics and kinetics of Sb_4 on Ge(001) surface with biaxial strain using DFT calculations. They show sensitive dependence on the strain state of the substrate: in the absence of an external strain, Sb_4 dissociates via a *square* intermediate state with a *bond-twisting assisted rigid rotation* mechanism for the first-stage conversion and a *substrate-dimer-bond-breaking assisted piecewise rotation dissociation* pathway across the dimer row for the second-stage conversion. While with an applied strain, the energetics and kinetics can be qualitatively altered, leading to distinct reaction pathways and patterns due to the weak interactions between Ge-Ge and Sb-Ge bonds. For comparison, we also performed calculations for Sb_4 on Si(001). In stark contrast to the case of Sb_4 on Ge(001), the external strain has little effect on the dissociation behavior on Si(001) due to the strong interactions between Sb-Si and Si-Si bonds.

The reported calculations are carried out using VASP code[19] with ultrasoft pseudopotentials[20] and the generalized gradient approximation (GGA).[21] An energy cutoff of 200 eV for the plane-wave basis set is used. The supercell size is set to $XYZ=16\times32\times35.72$ Å^3 with ten layers of Ge in the Z direction and one layer of hydrogen to passivate the bottom Ge layer. The XY plane corresponds to a 4×8 slab with periodic boundary conditions. In all the calculations, the top seven layers of Ge are fully relaxed, while the bottom three are fixed at the bulk structure. The energy minimization is done over the atomic and electronic degrees of freedom using the conjugate gradient iterative technique with two k points in the surface Brillouin zone.

All of the results reported in this Brief Report are obtained at 0 K. In this case, the most stable $c(4\times2)$ surface is selected as a model, although the Ge(001)-$c(4\times2)$ and $p(2\times1)$ surfaces coexist in a wide range of temperatures.[5] On the anisotropic dimeric surface, we consider eight types of Sb_4 clusters shown in Fig. 1. Here, T_A and T_B describe 3D tetrahedral clusters with different adsorption directions on the dimer row; R is a *rhombuslike* cluster with the long axis along the surface dimer rows; P is a *rotated rhombus* cluster with the long axis perpendicular to the surface dimer rows; S is a square tetramer on the dimer row; S_A is a *rectanglelike* cluster, half on the dimer row and half over the trough; and AA and BB (or AB) consist of a pair of loosely coupled type A and B dimers in each case. The binding energy of these configurations defined as $E_n=E[n]-E[0]$, where $E[n]$ and $E[0]$ are the total energy of the system with and without n Sb adatoms on the Ge(001) or Si(001)-$c(4\times2)$ surface.

Our calculations have revealed different stability sequences (see Fig. 1): $T_B<P<R<BB<T_A<AA<S\leq S_A$ on Ge(001) and $T_B<T_A<P<S_A<S<R<BB<AA$ on Si(001). Moreover, the binding energies of Sb_4 on Ge(001) are consistently smaller than the corresponding values on Si(001), indicating weaker interactions between the Sb_4 molecule and the surface atoms on Ge(001). These energetic results help explain that Sb_4 on Si(001) tend to form AA type structure as a pair of dimers,[2–4,14] while Sb_4 on Ge(001) favor to form S or S_A type clusters.[5] The detailed structural information such as bond distances have been reported by Martínez-Guerra *et al.*[13] and are omitted here.

Our primary objective here is to examine the effect of external strain on the relative stability of various configurations of Sb_4 molecules. The idea is to check whether a tensile (+2%)/compressive(−2%) strain on Si/Ge surfaces that would bring their lattice parameters closer to each other would also have a similar effect on the cluster dissociation behavior. Our calculations show (see Fig. 1) that, under ap-

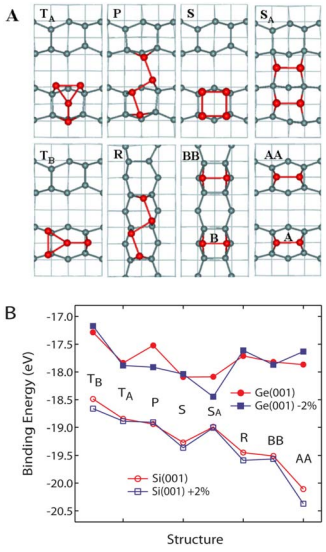

FIG. 1. (Color online) (a) Optimized cluster configurations for Sb_4 on Ge(001) and Si(001). Large (red) and small (gray) circles represent Sb and top-two-layer Ge (or Si) atoms, respectively. Lines are drawn to indicate the chemical bonds. (b) The binding energy of these configurations defined as $E_n = E[n] - E[0]$, where $E[n]$ and $E[0]$ are the total energy of the system with and without n Sb adatoms on the Ge(001) or Si(001)-$c(4\times2)$ surface. The surface lattice parameters denoted in the figures are 4.00 Å for Ge(001), 3.92 Å for Ge−2%, and Si+2%, and 3.84 Å for Si(001), respectively.

plied strain, the energetics of various configurations on Ge(001) shows significant changes and makes state P and S_A more stable. Meanwhile, the strain-induced lattice expansion does not produce any appreciable changes for the energetics (and kinetics, see below) of Sb_4 on Si(001). So the naive expectation that smaller lattice constant of the strained Ge(001) may bring the relative energetics of Sb_4 closer to that on Si(001) does not materialize here. These energetics results provide a basis for understanding the relative stability of the Sb_4 molecules; but to explain the diverse dissociation pathways and patterns, a critical next step is to examine the energy barriers (i.e., kinetics) of various reaction pathways.

Based on the experimental observations for Sb_4 on Ge(001) and Si(001),[2–5] we have performed large-scale calculations to search for optimal pathways for Sb_4 state conversion through a stepwise procedure that maps out the potential-energy surface using a 11×11 grid mesh as illustrated in Fig. 2(a) for the T_A, $T_B \rightarrow S$ conversion on Ge(001). Throughout the reaction pathway, the top seven layers of Ge (Si) and Sb_4 are fully relaxed. All the calculated data are shown in Table I with available experimental data for Sb_4 on Si(001).[4] We observe rich dynamics of bonding between the adatoms and substrate atoms in the T_A, $T_B \rightarrow S$ conversion processes with a bond-twisting assisted rigid rotation mechanism [Fig. 2(d)]. For example, for $T_A \rightarrow S$, it proceeds initially from $T_A \rightarrow T_{A2}$ with the breaking of the bond between atoms 1–3 and the twisting of bond 3–4, while simultaneously a new bond between atoms 3–5 is formed. It is followed, from $T_{A2} \rightarrow S$, by the formation of two new bonds 1–3 and 2–4, completing cluster S. Similar behavior is found for the $T_B \rightarrow S$ pathway. From $T_B \rightarrow T_{B2}$ with the twisting rotation of bond 3–4, bond 4–5 is broken and a new bond 3–5 is formed and then from T_{B2} to S with the formation of a new bond between atoms 2–4. Similar multistep bond breaking and forming processes are also observed for $T_A \rightarrow P$ and $T_B \rightarrow R$ [see Fig. 2(e)].

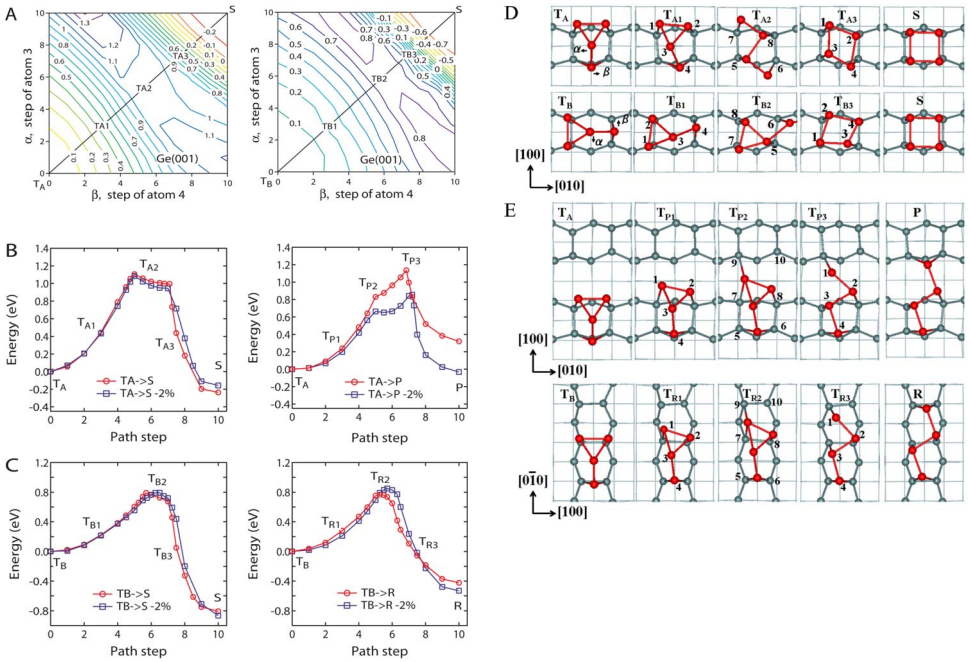

FIG. 2. (Color online) Strain dependent first-stage (3D-to-2D flat tetramers) conversion pathways of Sb_4 on Ge(001). (a) Potential-energy surface for $T_A \rightarrow S$ and $T_B \rightarrow S$, generated by a 11×11 grid mesh; (b) energy profiles for $T_A \rightarrow S$ compared to $T_A \rightarrow P$; (c) energy profiles for $T_B \rightarrow S$ compared to $T_B \rightarrow R$; and [(d) and (e)] illustration of the above dissociation pathways. The atoms labeled 1–4 correspond to the Sb_4 molecule and 5–10 correspond to Ge atoms on the surface.

TABLE I. Calculated energy barriers (in eV) for Sb tetramers on Ge(001) and Si(001) compared to available experimental data (in parentheses) for Sb on Si(001) (Ref. 4).

Path	Ge(001)	Ge(001)−2%	Si(001)	Si(001)+2%
$T_A \rightarrow S$	1.09	1.08	1.14	1.11
$T_A \rightarrow P$	1.13	0.86	0.83(0.7±0.1)	0.85
$T_B \rightarrow S$	0.79	0.81	0.93	0.99
$T_B \rightarrow R$	0.77	0.85	0.55	0.57
$S \rightarrow S_A$	1.08	0.92		
$S_A \rightarrow AA$	0.95	1.40		
$S \rightarrow BB$	1.40	1.34		
$P \rightarrow S_A$	0.87	0.88	1.01	1.13
$P \rightarrow AB$	0.81	0.93	0.92(0.9±0.1)	1.04

In the first-stage (3D-to-2D flat tetramer) conversion, there are two pairs of competing reaction pathways: $T_A \rightarrow P$ vs $T_A \rightarrow S$ and $T_B \rightarrow R$ vs $T_B \rightarrow S$. For Sb_4 on Ge(001) (see Fig. 2), the energy barriers are 1.13 eV for $T_A \rightarrow P$ and 0.77 eV for $T_B \rightarrow R$, which are almost the same as 1.09 eV for $T_A \rightarrow S$ and 0.79 eV for $T_B \rightarrow S$, respectively. Here the energetics favors $T_A \rightarrow S$ and $T_B \rightarrow S$ pathways. On the other hand, for Sb_4 on Si(001) (see Fig. 3), larger energy barriers of 1.14 eV for $T_A \rightarrow S$ and 0.93 eV for $T_B \rightarrow S$ than the barriers of 0.83 eV for $T_A \rightarrow P$ and 0.55 eV for $T_B \rightarrow R$ are obtained. Consequently, $T_A \rightarrow P$ is favored by the kinetics (small barrier) although S is lower in energy than P; meanwhile the $T_B \rightarrow R$ pathway is preferred by both kinetics and energetics.

We now turn to the effect of biaxial compressive strain on Ge(001) surface. For T_A on Ge(001) under a −2% compression, structure P becomes more stable (than T_A) and the barrier for $T_A \rightarrow P$ is decreased from 1.13 to 0.86 eV, which is smaller than the barrier of 1.08 eV for $T_A \rightarrow S$. Consequently, kinetics favors $T_A \rightarrow P$ pathway although S is lower in energy

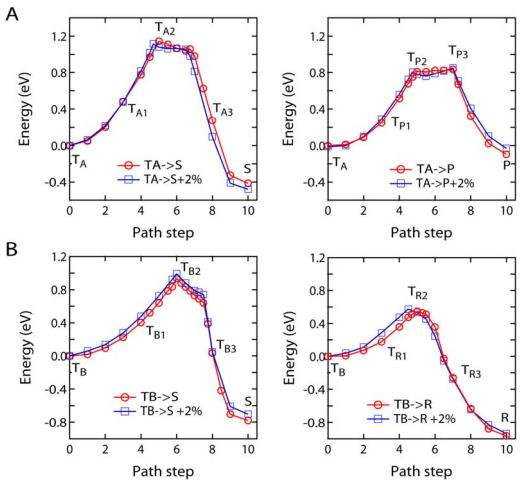

FIG. 3. (Color online) Strain dependent first-stage (3D-to-2D flat tetramers) conversion pathways of Sb_4 on Si(001). (a) Energy profiles for $T_A \rightarrow S$ compared to $T_A \rightarrow P$; (b) energy profiles for $T_B \rightarrow S$ compared to $T_B \rightarrow R$. For the corresponding pathways see Figs. 2(d) and 2(e).

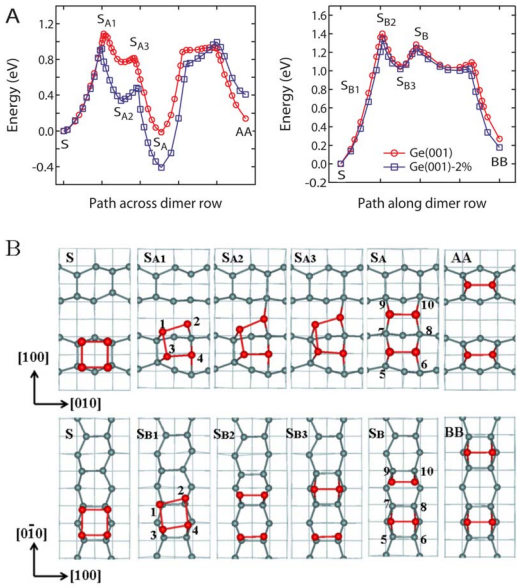

FIG. 4. (Color online) Strain dependent second-stage (2D tetramer-to-dimer) conversion pathways of the square tetramer Sb_4 on Ge(001). (a) Energy profiles for $S \rightarrow AA$ compared to $S \rightarrow BB$; (b) illustration of the above dissociation pathways.

than P. For T_B on Ge(001) under a −2% compression, the pathways $T_B \rightarrow S$ and $T_B \rightarrow R$ have nearly the same energy barrier; the energetics dictates that $T_B \rightarrow S$ is favored. On the other hand, for T_A and T_B on Si(001) (see Fig. 3), the external strain does not have any significant effect on either the energy barrier or the relative total energy to change the reaction pathway. These results show that the Sb_4 precursor dissociation pathways on Ge(001) can be effectively altered by external strain, which is likely caused by the relatively weak interaction between the Sb-Ge and Ge-Ge bondings. Meanwhile, the tetramer dissociation behavior on Si(001) remains robust even under a large external tensile strain up to 4%; this reflects the influence of the strong interaction between Sb-Si and Si-Si bondings in comparison to Sb-Ge and Ge-Ge bonds.

Next we consider the second-stage (2D tetramer-to-dimer) dissociation pathways from S to AA and BB on Ge(001). The energy profile and the corresponding reaction pathway are shown in Fig. 4. For $S \rightarrow AA$ across the dimer row, we identify a *piecewise rotation pathway* from S to S_A with two *substrate-dimer-bond breaking*. Adatom 2 first moves from S to S_{A2} across the dimer row with the breaking of the bonds between atoms 2–4, 6–8, and a concurrent formation of a new bond 2–10. Then, along $S_{A2} \rightarrow S_A$, adatom 1 moves across the dimer row by a sequential breaking of the 1–3, 5–7 bonds, and the simultaneous formation of the 1–9 bond, completing the *piecewise rotation* process. The energy barrier for this piecewise rotation process is 1.08 eV that is reduced from 1.32 eV for direct transformation from S to S_A by moving ad-dimer 1–2 rigidly. Such *substrate-dimer-bond-breaking assisted piecewise dissociation* is favored on Ge(001) due to the weak interaction of Ge-Ge bonds. From S_A to AA, adatoms 1 and 2 move toward the adjacent dimer row with a *rolling-over* pathway with an energy barrier of 0.95 eV. The calculated energetics and barriers shown in

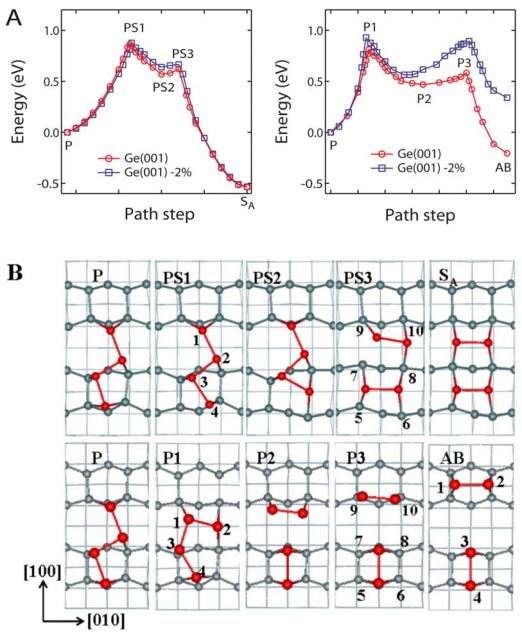

FIG. 5. (Color online) Strain dependent second-stage conversion pathways of the rotated rhombus Sb_4 on Ge(001). (a) Energy profiles for $P \rightarrow S_A$ compared to $P \rightarrow AB$ on Ge(001); (b) illustration of the above reaction pathways.

Fig. 4 also suggest that the conversions among S, S_A, and AA are reversible when no external strain is present; it is in good agreement with the experimental observation.[5] When a compressive strain is applied to Ge(001), the barrier for S to S_A decreases significantly; at the same time, the energy of S_A is also lowered. Meanwhile, the barrier from S_A to AA is significantly increased and the energy of AA is raised [see Fig. 4(a)]. As a result, S_A is stabilized under compressive strain by both kinetics (lower barrier from S) and energetics (lower total energy). On the other hand, it is seen that the splitting along the dimer row from $S \rightarrow BB$ shows a large energy barrier of 1.40 eV and the related energetics and barrier are not very sensitive to strain to change the pathway.

It is also interesting to note that there is a strain-induced competing reaction pathways $P \rightarrow S_A$ vs $P \rightarrow AB$ as shown in Fig. 5. The pathway $P \rightarrow AB$ is found for Sb_4 on Si(001) (Refs. 4 and 14) but unfavorable for Sb_4 on Ge(001) due to higher energy of the AB states. As a result, a divergent pathway $P \rightarrow S_A$ is preferred under compressive strain by both kinetics and energetics. Throughout this $P \rightarrow S_A$ process, another substrate-dimer-bond-breaking assisted piecewise dissociation pathway is proposed [see Fig. 5(b)]. We first move atom 4 along the dimer row (010 direction) from P to PS2 with the 3–4 dimer bond rotation and then move atom 1 from step PS2 to S_A to rotate the 1–2 dimer bond. This substrate-dimer-bond-breaking assisted process is unfavorable on Si(001) due to the strong bonding of Si-Si dimer.

Lastly, we discuss the finite temperature conversion behavior. The conversion rate (λ) between two states can be estimated by $\lambda = \lambda_0 e^{(-E_b/k_B T)}$, where λ_0 is the prefactor, E_b is the energy barrier, k_B is the Boltzmann constant, and T is the temperature. Based the sequence of STM images reported by Chan and Altman[5] and the energy barrier (see Table I), the prefactor for Sb_4 on Ge(001) is estimated to be 10^{11}–10^{13}, in contrary to 10^7–10^9 s^{-1} for Sb_4 on Si(001) as reported by Mo.[4] We can see that conversion prefactor for Sb_4 on Ge(001) is about 10^4 times larger than that for Sb_4 on Si(001) due to the different bonding nature of Sb-Ge and Sb-Si. As a result, the thermal annealing temperatures should be expected to be 300 to 520 K for Sb_4 on Ge(001) and 330 to 620 K for Sb_4 on Si(001) in the conversion rate range of 1–10.

In summary, our DFT calculations reveal sensitive strain selection of the first-stage (3D-to-2D flat tetramer) and second-stage (2D tetramer-to-dimer) dissociation pathways of antimony precursors on Ge(001). These pathways are indeed governed by a variety of energetics and kinetics conditions with substrate-dimer-bond breaking due to the weak interactions between Sb-Ge and Ge-Ge bonds. They exhibit strong anisotropic reaction channels across the dimer row and are controllable by external strain, leading to distinct dimer patterns. Meanwhile, the strain-induced lattice expansion does not produce any appreciable changes for the energetics and kinetics of Sb_4 on Si(001) due to the stronger interactions between Sb-Si and Si-Si bonds. These results provide an excellent account for experimental observations[2–5] and can be used as a basis for describing the surfactant effect in Sb-mediated epitaxial growth of Ge on Si(001).[18]

This study was supported by the NSFC and MOST of China. Changfeng Chen was supported by the U.S. Department of Energy. We are thankful to the crew of the Center for Computational Materials Science at IMR, Tohoku University for their support at the SR11000 supercomputing facilities.

*wjt@aphy.iphy.ac.cn

[1] J. V. Barth *et al.*, Nature (London) **437**, 671 (2005).
[2] Y. W. Mo, Phys. Rev. Lett. **69**, 3643 (1992).
[3] Y. W. Mo, Science **261**, 886 (1993).
[4] Y. W. Mo, Phys. Rev. B **48**, 17233 (1993).
[5] L. H. Chan and E. I. Altman, Phys. Rev. B **63**, 195309 (2001).
[6] S. B. Zhang *et al.*, Phys. Rev. Lett. **87**, 166104 (2001).
[7] W. E. McMahon *et al.*, Phys. Rev. Lett. **89**, 076103 (2002).
[8] M. Kawamura *et al.*, Phys. Rev. Lett. **91**, 096102 (2003).
[9] O. Kubo *et al.*, Appl. Surf. Sci. **169-170**, 93 (2001).
[10] J. H. G. Owen *et al.*, J. Mater. Sci. **41**, 4568 (2006).
[11] J. H. G. Owen *et al.*, Phys. Rev. Lett. **88**, 226104 (2002).
[12] J. T. Wang *et al.*, Phys. Rev. B **67**, 193307 (2003); J. T. Wang *et al.*, Phys. Rev. Lett. **94**, 226103 (2005).
[13] E. Martínez-Guerra *et al.*, Phys. Rev. B **73**, 075302 (2006).
[14] J. T. Wang *et al.*, Phys. Rev. Lett. **97**, 046103 (2006).
[15] M. Copel *et al.*, Phys. Rev. Lett. **63**, 632 (1989).
[16] A. Portavoce *et al.*, Phys. Rev. B **69**, 155416 (2004).
[17] N. Paul *et al.*, Phys. Rev. Lett. **98**, 166104 (2007).
[18] En-Zuo Liu *et al.*, Phys. Rev. B **76**, 193301 (2007).
[19] G. Kresse and J. Furthmüller, Comput. Mater. Sci. **6**, 15 (1996).
[20] D. Vanderbilt, Phys. Rev. B **41**, 7892 (1990).
[21] J. P. Perdew and Y. Wang, Phys. Rev. B **45**, 13244 (1992).